

# Raman scattering study of the high temperature phase transitions of NaTaO<sub>3</sub>

Nayara G. Teixeira<sup>a</sup>, Anderson Dias<sup>b</sup>, R.L. Moreira<sup>a,\*</sup>

<sup>a</sup> Departamento de Física, ICEx, UFMG, C.P. 702, Belo Horizonte MG 30123-970, Brazil

<sup>b</sup> Departamento de Química, ICEB, UFOP, Ouro Preto MG 35400-000, Brazil

Available online 9 March 2007

## Abstract

The phase transition sequence of sodium tantalate (NaTaO<sub>3</sub>) ceramic samples has been investigated by Raman spectroscopy, from room temperature up to 640 °C. At room temperature, NaTaO<sub>3</sub> shows an orthorhombically distorted perovskite structure belonging to the *Pbnm* space group. Raman and infrared vibrational spectra at 20 °C are in relative good agreement with group theory predictions for this group. At high temperatures, NaTaO<sub>3</sub> shows three phase transitions, in the sequence *Pbnm* (~450 °C) *Cmcm* (~560 °C) *P4/mbm* (~620 °C) *Pm3m*. The Raman spectra for the two intermediate high temperature phases showed a decreasing of the number of the active modes, accompanied by band broadening, and were well compatible with structural symmetry increasing at higher temperatures.

© 2007 Elsevier Ltd. All rights reserved.

**Keywords:** Sintering; Spectroscopy; Dielectric properties; Perovskites; Capacitors

## 1. Introduction

At room temperature, NaTaO<sub>3</sub> belongs to the family of orthorhombically distorted perovskites with GdFeO<sub>3</sub>-type structure, which has been determined as *Pbnm* (*Z*=4).<sup>1,2</sup> This structure rules out the possibility of ferroelectricity for this compound, claimed previously by some authors,<sup>3,4</sup> and showed by similar materials like NaNbO<sub>3</sub><sup>5,6</sup> and BiInO<sub>3</sub>.<sup>7</sup> The centrosymmetrical nature of NaTaO<sub>3</sub> was also confirmed by the absence of characteristic dielectric anomalies in a very large temperature interval and of polarization loops in ceramics and single crystals.<sup>8</sup> On the other hand, optical, dielectric and calorimetric measurements<sup>8–10</sup> denoted the presence of three phase transitions (PT) in the high temperature region. These transitions were confirmed by Kennedy et al.<sup>11</sup> and Darlington and Knight,<sup>12</sup> who also determined the structure of the three high temperature phases, with good agreement between their independent neutron diffraction results. According to Ref. 11, the PT sequence of NaTaO<sub>3</sub> would be *Pbnm* (~447 °C) *Cmcm* (~562 °C) *P4/mbm* (~617 °C) *Pm3m*. Although there exist several ABO<sub>3</sub> compounds with the same hettotype (*Pbnm*) and aristotype (*Pm3m*) groups, at least five different PT sequences have been identi-

fied between these phases, as described by Knight et al.<sup>13</sup> Thus, the particular PT sequence of NaTaO<sub>3</sub> deserves more investigation; in particular, by using vibrational spectroscopic techniques, since, at our knowledge, there is no spectroscopic report for any of the proposed phases to date.

Besides its interesting high temperature PT sequence, NaTaO<sub>3</sub> attracts our attention because it attains the highest photocatalytic quantum yield for water splitting into H<sub>2</sub> and O<sub>2</sub> under UV irradiation among all known materials, exceeding 50%, when doped with La.<sup>14–16</sup> Therefore, spectroscopic data could also be useful for photodynamic investigations, as well as for structural studies. In this work, Raman scattering and infrared reflectivity techniques have been used in order to determine the main phonon modes of hydrothermally prepared NaTaO<sub>3</sub> ceramics. The number of observed vibrational bands and the selection rules for Raman and infrared modes confirm the proposed room temperature structure. Raman spectroscopy was then used to investigate the phonon evolution in the three high temperature phases.

## 2. Experimental

NaTaO<sub>3</sub> was obtained from stoichiometric amounts of analytical grade reagents NaOH and TaCl<sub>5</sub>. After dissolution of each reagent in deionised water (18.2 MΩ cm), they were mixed under stirring and pH 13. Conventional hydrothermal syntheses were

\* Corresponding author. Tel.: +55 31 3499 5624; fax: +55 31 3499 5600.  
E-mail address: [bmoreira@fisica.ufmg.br](mailto:bmoreira@fisica.ufmg.br) (R.L. Moreira).

performed in 2 L floor stand reactors equipped with turbine-type impellers and digital temperature controllers at 200 °C (10 bar), for 2 h. The powders were uniaxially pressed at 110 MPa into cylindrical discs of 5 mm height and 15 mm diameter. The sintering occurred in a covered alumina crucible at 1400 °C, for 4 h. The obtained ceramics were dense, showing experimental densities above 93% of the theoretical value. X-ray powder diffraction performed in a Philips PW1830 diffractometer with Cu K $\alpha$  radiation (40 kV, 30 mA) and graphite monochromator, from 10° to 100° 2 $\theta$  at a speed of 0.02° 2 $\theta$ /s, showed good agreement with the corresponding ICDD #74-2478 card, with no indication of impurities or secondary phases. The dielectric response in the kHz-to-MHz region was measured with a HP4192A impedance analyzer. The obtained results were  $\epsilon = 25$  and  $\tan \delta < 10^{-2}$  (at 1 MHz).

Raman spectra were collected in back-scattering configuration by using an Olympus microscopy attached to a Dilor XY spectrometer (objective 10 $\times$ , 12 mm focal distance). The 514.5 nm line of an Ar<sup>+</sup> laser (10 mW) was used as exciting line and a CCD as detector. The spectral resolution was better than 2 cm<sup>-1</sup> and the accumulation times were typically four collections of 120 s. The sample was put in an optical furnace with temperature control ( $\pm 1$  °C) and the measurements were taken during the heating cycle. The obtained spectra were divided out by the Bose factor<sup>17</sup> before being fitted by a sum of Lorentzian lines. Fourier-transform infrared reflectivity measurements were conducted under vacuum (10<sup>-4</sup> bar) in a BOMEM-DA8 spectrometer, equipped with a fixed-angle specular reflectance accessory (external incidence angle of 11.5°), at 4 cm<sup>-1</sup> of spectral resolution, with 64 scans. The spectra were recorded using a Globar source, a 6  $\mu$ m coated Mylar hypersplitter<sup>®</sup>, and a liquid-helium-cooled silicon bolometer. As reference spectrum we used a “rough” mirror, obtained by coating a thin gold film onto one of the sample’s surface.

### 3. Results and discussions

It is now accepted that NaTaO<sub>3</sub> belongs to the centrosymmetric *Pbnm* space group.<sup>11,12</sup> In this structure, Ta ions occupy 4*b* Wyckoff-site of *C*<sub>1</sub> symmetry, Na and O(1) ions occupy 4*c* sites of *C*<sub>s</sub><sup>xz</sup> symmetry and O(2) ions occupy 8*d* sites of general *C*<sub>1</sub> symmetry. The site group method of Rousseau et al.<sup>18</sup> leads to the following decomposition of the 60 degrees of freedom of the vibration modes at the Brillouin zone centre into its irreducible representations (i.r.):  $\Gamma = 7A_g + 8A_u + 5B_{1g} + 10B_{1u} + 7B_{2g} + 8B_{2u} + 5B_{3g} + 10B_{3u}$ . Therefore, for unpolarised spectra of a ceramic sample, we would expect at most 24 Raman bands ( $7A_g + 5B_{1g} + 7B_{2g} + 5B_{3g}$ ) and 25 infrared-active ones ( $9B_{1u} + 7B_{2u} + 9B_{3u}$ ). The Raman spectrum of NaTaO<sub>3</sub> at room temperature (RT) is presented in Fig. 1. After fitting, we could discern 21 bands (although some of them, which are very weak and broad, could be combination modes), whose positions and widths are summarised in Table 1. The agreement between the predicted and observed number of fundamentals is quite good, considering that modes belonging to different i.r. cannot be resolved by unpolarised spectroscopy of unoriented ceramics. It is also worthy noticing the peak

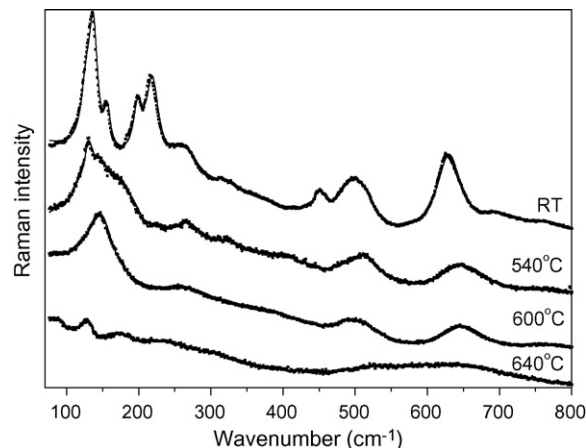


Fig. 1. Micro-Raman spectra (circles) of NaTaO<sub>3</sub> ceramics fitted by sum of Lorentzian lines (solid curves). The room temperature (RT) and the high-temperature spectra into each different structural phase are vertically offset.

splitting of the TaO<sub>6</sub> octahedra mode above 550 cm<sup>-1</sup> into several bands (the five or six higher frequency bands), due to the multiple numbers of ions into the unit cell. The same feature occurs relatively to the other regions of the spectra, i.e., we can clearly identify groups of bands in the regions 60–240 cm<sup>-1</sup> (six Na translations), 240–400 cm<sup>-1</sup> (three TaO<sub>6</sub> bending modes) and 400–520 cm<sup>-1</sup> (six TaO<sub>6</sub> rotation or tilting modes).

Let us now analyse the RT infrared-reflectivity spectrum of the NaTaO<sub>3</sub> ceramics, presented in Fig. 2. The experimental spectrum was fitted by an expression based upon the four-parameter semi-quantum model,<sup>19</sup> using a non-linear least-square program<sup>20</sup> and the fitting parameters are presented as an

Table 1  
Observed Raman bands for NaTaO<sub>3</sub>, into the orthorhombic (RT = 20 and 540 °C) and tetragonal (600 °C) phases

20 °C	540 °C	600 °C
125/16	134/30	
135/18	146/12	
156/9	153/15	160/30
187/10	168/25	
198/12	186/25	
217/21	231/12	
261/42	268/34	270/40
322/34	323/52	
362/43	369/43	
431/30	404/25	
448/11		
454/15	472/42	
485/24		490/40
501/32		
516/15	512/55	
572/20		
620/22		
628/27		
642/36	647/45	647/62
697/45	680/30	
<sup>a</sup> 767/60	<sup>a</sup> 756/50	<sup>a</sup> 770/60

Positions/widths (full-widths at half maximum) obtained by fitting the experimental data with Lorentzian lines (in cm<sup>-1</sup>).

<sup>a</sup> Possibly second order.

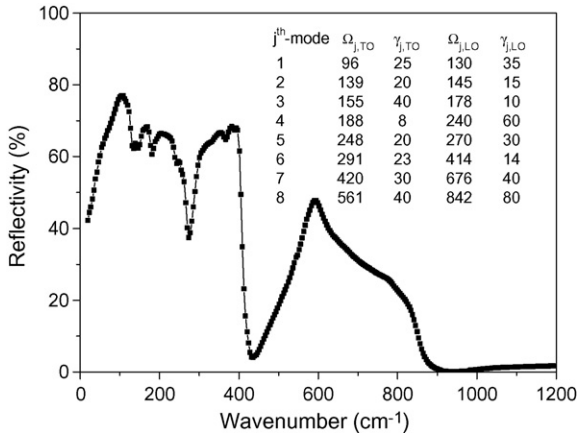


Fig. 2. Infrared reflectance spectra of the NaTaO<sub>3</sub> sample at RT. Inset: dispersion parameters calculated from the fit of the experimental spectrum by the factorized form of the dielectric permittivity.<sup>19</sup> The positions ( $\Omega$ ) and damping constants ( $\gamma$ ) are given in cm<sup>-1</sup>.

inset in Fig. 2. The number of depicted infrared modes listed in Fig. 2 (eight) is much lower than the 25 ones predicted by group theory. The reasons for this discrepancy are linked to: (i) the unoriented nature of polycrystalline ceramics, (ii) the fact that the RT phase is derived from higher symmetry phases and (iii) the complex dependence of the optical reflectance on the phonon parameters.<sup>19,20</sup> Indeed, the symmetry rules for modes belonging to the different i.r. cannot be explored in ceramic systems. In the present case, where the orthorhombic structure was obtained from small distortions from the cubic parent phase, we expect that several modes of different i.r. of the low temperature phase come from the same i.r. of the parent phase (because of the increasing volume of lower temperature phases). However, the four-parameter semi-quantum model<sup>19</sup> do not allow one to discern modes with close TO and LO frequencies (the TO frequency of any mode except the ( $j^{\text{th}} + 1$ ) mode must be higher than the LO value of the  $j^{\text{th}}$  mode). In other words, each linearly independent infrared-active i.r. should be described by an independent factorized equation for the dielectric permittivity.<sup>19</sup> Only in this case and by measuring polarised infrared spectra of single crystals the quasi-degenerated states can be resolved.

Although the infrared results showed here were poor in terms of studying the correctness of the room temperature space group of NaTaO<sub>3</sub>, they give useful information as: they agree with a centrosymmetrical group for this phase, since Raman and infrared modes are mutually exclusive (otherwise the Raman bands would be very large – for each observed infrared mode there would be a Raman band going from the TO to the corresponding LO branch); it was possible to obtain the electronic ( $\epsilon_{\infty} = 2.5$ ) and phononic ( $\epsilon_0 - \epsilon_{\infty} = 37.5$ ) contributions to the dielectric constant; they allowed us to estimate the intrinsic quality factor,  $Q_f = f/\tan \delta = 14,000$  GHz, at microwave frequencies.<sup>21</sup> This  $\epsilon_0$  value can be compared with the values showed in Ref. 8 for Nb doped NaTaO<sub>3</sub> (ca. 100) and with our measurements on pure samples (25), obtained at the MHz range. The relatively high  $\epsilon_0$  value was surely responsible for the first attributions of this material as ferroelectric. It is worthy noticing that the main contribution for the dielectric response comes

from the lower frequency phonon mode, i.e., from dipole polarization due to the movements of the Na ion into the lattice. Concerning the high intrinsic  $Q_f$  value, it could be interesting to evaluate the potential use of this material for microwave applications. On the other hand, the very low radio-frequency Q value ( $\sim 10^2$  at 1 MHz) indicates that extrinsic losses due to space charges, impurities, grain boundaries and imperfections are very important in this system, and therefore, that sample purity and morphology should be improved before aiming any applications.

Since the Raman technique was successfully applied to investigate the optical phonon modes of NaTaO<sub>3</sub> ceramics at room temperature, we have collected the Raman spectra into the high temperature phases, also showed in Fig. 1 (besides the RT spectrum). It is worthy noticing that into each phase the bands generally present a normal thermal behavior, i.e., softening and broadening with increasing temperature. However, a detailed study of these modes behavior, including some specific anomalous cases, as well as soft mode behavior near the phase transitions are beyond the scope of this work and will be presented elsewhere. All the spectra presented in Fig. 1 were taken into the same experimental condition, so that a direct comparison of their intensities is allowed. In the high temperature spectra we were able to identify 15 bands in the spectrum at 540 °C (*Cmcm* phase), 5 bands at 600 °C (*P4/mbm*) and “none” at 640 °C (*Pm3m*). Indeed, the later spectrum presents very broad and weak features, which are well compatible with the combination (second order) bands proposed by Perry and Tornberg,<sup>22</sup> for cubic Na<sub>x</sub>K<sub>1-x</sub>TaO<sub>3</sub> mixed crystals (extrapolated to  $x \rightarrow 1$ ). The results of our fittings by Lorentzian lines for the two intermediate phases are presented in Table 1. We can compare the number of observed bands with the group theory predictions by the factor group method<sup>18</sup> using the atomic positions of Refs. 11 and 12 which give, respectively, 24 ( $7A_g + 7B_{1g} + 4B_{2g} + 6B_{3g}$ ), 5 ( $A_{1g} + A_{2g} + B_{1g} + B_{2g} + E_g$ ) and 0 Raman-active modes, for the three high temperature phases of our system.

The absence of Raman fundamentals in the parent phase confirms its proposed ideal cubic symmetry. Concerning the other phases, we remark first that the PT are linked to octahedra tiltings around the crystallographic axes.<sup>11,12</sup> This is particularly important for the two ferroelastic transitions at higher temperatures: from cubic to tetragonal and from tetragonal to orthorhombic (*Cmcm*) phases, because the volume of the primitive cell doubles in each transition, increasing the number of active modes. However, in the case of the non-ferroelastic (lower temperature) phase transition, the same type of modes are seen with minor changes in both orthorhombic phases, although features of the same type of vibration tend to merge at higher temperatures.

#### 4. Conclusions

Raman scattering and infrared reflectance spectroscopic analyses of NaTaO<sub>3</sub> ceramics were done at RT. The observed Raman modes are in good agreement with group theory predictions for the assumed structure. The number of observed polar phonon modes was lower than predicted, but since the main modes were determined, it was possible to estimate the intrinsic dielectric response of the material in the microwave region.

High-temperature Raman spectra showed the phonon evolution in the three high temperature phases of NaTaO<sub>3</sub>. The changes are minor for the lowest temperature PT with non-ferroelastic nature and major for the two ferroelastic higher temperature PT (for tetragonal and cubic systems). At 640 °C, the Raman fundamentals tend to disappear, as expected for an ideal cubic perovskite structure.

### Acknowledgements

The authors thank Prof. Marcos A. Pimenta for the use of his Raman facilities, and the financial support of MCT/CNPq and FAPEMIG.

### References

- Marezio, M., Remeika, J. P. and Dernier, P. D., The crystal chemistry of the rare earth orthoferrites. *Acta Cryst. B*, 1970, **26**, 2008–2022.
- Ahtee, M. and Unonius, L., The structure of NaTaO<sub>3</sub> by X-ray powder diffraction. *Acta Cryst. A*, 1977, **33**, 150–154.
- Matthias, B. T., New ferroelectric crystals. *Phys. Rev.*, 1949, **75**, 1771.
- Kay, H. F. and Miles, J. L., The structure of cadmium titanate and sodium tantalate. *Acta Cryst.*, 1957, **10**, 213–218.
- Darlington, C. N. W. and Megaw, H. D., The low-temperature phase transition of sodium niobate and the structure of the low-temperature phase. *N. Acta Cryst. B*, 1973, **29**, 2171–2185.
- Lanfredi, S., Lente, M. H. and Eiras, J. A., Phase transition at low temperature in NaNbO<sub>3</sub> ceramic. *Appl. Phys. Lett.*, 2002, **80**, 2731–2733.
- Belik, A. A., Stefanovich, S. Y., Lazoryak, B. I. and Takayama-Muromachi, E., BiInO<sub>3</sub>: a polar oxide with GdFeO<sub>3</sub> perovskite structure. *Chem. Mater.*, 2006, **18**, 1964–1968.
- Iwasaki, H. and Ikeda, T., Studies on the system Na(Nb<sub>1-x</sub>Ta<sub>x</sub>)O<sub>3</sub>. *J. Phys. Soc. Jpn.*, 1963, **18**, 157–163.
- Cross, L. E., A thermodynamic treatment of ferroelectricity and anti-ferroelectricity in pseudo-cubic dielectrics. *Phil. Mag.*, 1956, **1**, 76–92.
- Aleksandrowicz, A. and Wojcik, K., Electrical properties of single-crystals and ceramic samples of NaTaO<sub>3</sub>. *Ferroelectrics*, 1989, **99**, 105–113.
- Kennedy, B. J., Prodjosantoso, A. K. and Howard, C. J., Powder neutron diffraction study of the high temperature phase transitions in NaTaO<sub>3</sub>. *J. Phys. Condens. Matter*, 1999, **11**, 6319–6327.
- Darlington, C. N. W. and Knight, K. S., High-temperature phases of NaNbO<sub>3</sub> and NaTaO<sub>3</sub>. *Acta Cryst. B*, 1999, **55**, 24–30.
- Knight, K. S., Marshall, W. G., Bonanos, N. and Francis, D. J., Pressure dependence of the crystal structure of SrCeO<sub>3</sub> perovskite. *J. Alloys Compd.*, 2005, **394**, 131–137.
- Kato, H. and Kudo, A., New tantalate photocatalysts for water decomposition into H<sub>2</sub> and O<sub>2</sub>. *Chem. Phys. Lett.*, 1998, **295**, 487–492.
- Yamakata, A., Ishibashi, T.-A., Kato, H., Kudo, A. and Onishi, H., Photo-dynamics of NaTaO<sub>3</sub> catalysts for efficient water splitting. *J. Phys. Chem. B*, 2003, **107**, 14383–14387.
- He, Y., Zhu, Y. F. and Wu, N. Z., Synthesis of nanosized NaTaO<sub>3</sub> in low temperature and its photocatalytic performance. *J. Solid State Chem.*, 2004, **177**, 3868–3872.
- Hayes, W. and Loudon, R., *Scattering of Light by Crystals*. Wiley, New York, NY, 1978, pp. 7, 31.
- Rousseau, D. L., Bauman, R. P. and Porto, S. P. S., Normal mode determination in crystals. *J. Raman Spectrosc.*, 1981, **10**, 253–290.
- Gervais, F. and Echehut, P., In *Incommensurate Phases in Dielectrics*, ed. R. Blinc and A. P. Levanyuk. North Holland, Amsterdam, 1986, p. 337.
- Meneses, D. D., *IRFit2.0 Adjustment Program*. Orléans University, France, 1999 (desouza@cnsr-orleans.fr).
- Moreira, R. L., Feteira, A. and Dias, A., Raman and infrared spectroscopic investigations on the crystal structure and phonon modes of LaYbO<sub>3</sub>. *J. Phys. Condens. Matter*, 2005, **17**, 2775–2781.
- Perry, C. H. and Tornberg, N. E., Optical phonons in mixed sodium potassium tantalates. *Phys. Rev.*, 1969, **183**, 595–603.